ChemPubSoc Europe

DOI: 10.1002/cbic.201500518

CHEMBIOCHEM Full Papers

The Amyloid-Fibril-Forming Properties of the Amphibian Antimicrobial Peptide Uperin 3.5

Antonio N. Calabrese,[a] Yanqin Liu,[a, e] Tianfang Wang,[b, e] Ian F. Musgrave,[a] Tara L. Pukala,[a] Rico F. Tabor,[c] Lisandra L. Martin,*[c] John A. Carver,*[d] and John H. Bowie[a]

The amphibian skin is a vast resource for bioactive peptides, which form the basis of the animals' innate immune system. Key components of the secretions of the cutaneous glands are antimicrobial peptides (AMPs), which exert their cytotoxic effects often as a result of membrane disruption. It is becoming increasingly evident that there is a link between the mechanism of action of AMPs and amyloidogenic peptides and proteins. In this work, we demonstrate that the broad-spectrum amphibian AMP uperin 3.5, which has a random-coil structure in solution but adopts an α-helical structure in membrane-like environments, forms amyloid fibrils rapidly in solution at neutral pH. These fibrils are cytotoxic to model neuronal cells in a similar fashion to those formed by the proteins implicated in neurodegenerative diseases. The addition of small quantities of 2,2,2-trifluoroethanol accelerates fibril formation by uperin 3.5, and is correlated with a structural stabilisation induced by this co-solvent. Uperin 3.5 fibril formation and the associated cellular toxicity are inhibited by the polyphenol (−)-epigallocatechin-3-gallate (EGCG). Furthermore, EGCG rapidly dissociates fully formed uperin 3.5 fibrils. Ion mobility–mass spectrometry reveals that uperin 3.5 adopts various oligomeric states in solution. Combined, these observations imply that the mechanism of membrane permeability by uperin 3.5 is related to its fibril-forming properties.

Introduction

The majority of animals and plants have innate immune systems that comprise antimicrobial peptides (AMPs) as a vital component.[1] Often, upon receipt of a suitable stress stimulus, a range of AMPs with a spectrum of activities is secreted to ensure a fast, effective response against any invading microbe(s).[2] During the last 25 years, some 200 host-defence peptides have been isolated from the skin secretions of Australian frogs and toads. Many of these peptides are AMPs and/or have one or more neuropeptide-type activities.[3] This potent chemical arsenal ensures that the animal is effectively protected from the plethora of microbes that are rife in the hostile environment in which they live. The prevalence of AMPs in nature demonstrates their effectiveness as defence compounds, and their high activity and selectivity for microbes makes them an attractive starting point for the development of new peptide-based antimicrobials.[4]

AMPs often cause the death of microorganisms by interacting with the lipid bilayer and then causing membrane disruption in a specific, but not receptor-mediated, process.[1a,2] Several models have been proposed to describe this process of membrane permeabilisation.[4d,5] However, the finding that several AMPs have the ability to form β-sheet-rich amyloid fibril structures has led to the postulation that two seemingly unrelated classes of polypeptides, AMPs and fibril-forming (amyloidogenic) peptides, share common mechanisms of cytotoxicity through membrane disruption.[6]

The ability to form amyloid fibrils is proposed to be a generic property of all polypeptide sequences when they are subjected to the appropriate environmental and physicochemical stresses, with all amyloid fibrils sharing similar structural characteristics, irrespective of the protein from which they are derived.[7] A number of human diseases have the hallmark histological feature of extra- or intracellular amyloid deposits, including neurodegenerative diseases such as Alzheimer's and Parkinson's diseases, which are characterised by amyloid deposits of the amyloid β peptide (Aβ) and α-synuclein, respectively. Several mechanisms to rationalise the cytotoxicity of amyloidogenic species have been proposed, with the most toxic species postulated to be the oligomeric, pre-fibrillar aggregates,[8] which might function by forming pores in cellular membranes

[a] Dr. A. N. Calabrese, Dr. Y. Liu, Dr. I. F. Musgrave, Dr. T. L. Pukala, Prof. J. H. Bowie
School of Physical Sciences or School of Medical Sciences, The University of Adelaide
Adelaide, 5005, South Australia (Australia)

[b] Dr. T. Wang
Faculty of Science, Health, Education and Engineering, University of the Sunshine Coast
Sippy Downs 4556, Queensland (Australia)

[c] Dr. R. F. Tabor, Prof. L. L. Martin
School of Chemistry, Monash University
Clayton, 3800, Victoria (Australia)
E-mail: lisa.martin@monash.edu

[d] Prof. J. A. Carver
Research School of Chemistry, The Australian National University
Acton, 2601, Australian Capital Territory (Australia)
E-mail: john.carver@anu.edu.au

[e] Dr. Y. Liu, Dr. T. Wang
Present address: School of Technology, Hebei Agricultural University
Cangzhou, Hebei, 061100 (China)

Supporting information for this article is available on the WWW under http://dx.doi.org/10.1002/cbic.201500518.

in a similar way to AMPs.[9] The fibrils themselves are considered less cytotoxic or could in some cases be an inert, protective accumulation of the toxic species. However, in some cases, fibril cytotoxicity has been observed,[10] and fibril assembly on membranes can lead to cell death.[11] The largely unexplained cytotoxic mechanism of amyloid disease makes this field an active area of research, with numerous studies attempting to inhibit amyloid formation by use of small-molecule or peptide inhibitors.[12]

AMPs and amyloidogenic proteins share many structural and functional characteristics. These include their high affinities for negatively charged membranes, and a structural conversion from random-coil to α-helical secondary structure upon interacting with the membrane.[8c,13] In addition to some membrane-bound AMPs undergoing conversion to amyloid-like fibrils,[6] the amphibian AMP dermaseptin forms amyloid fibrils in solution.[14] The investigation of this novel relationship between AMPs and amyloid formation by disease-related proteins will potentially enable significant advances in understanding both amyloid diseases and the mechanism of action of AMPs.[15]

In this paper, we demonstrate that the 17-residue peptide uperin 3.5 (GVGDLIRKAVSVIKNIV-NH_2), a broad-spectrum AMP isolated from the skin secretions of the Australian toadlet *Uperoleia mjobergii,*[16] rapidly forms amyloid-like fibrils. By combining a variety of biophysical techniques, including thioflavin T (ThT) fluorescence, transmission electron microscopy (TEM) and ion mobility–mass spectrometry (IM-MS), insights have been gained into fibril formation by this peptide. We demonstrate that partial stabilisation of the α-helical secondary structure promotes fibril formation, and that the fibrils themselves share cytotoxic properties with amyloid species from the peptides and proteins implicated in neurodegenerative diseases. Fibril formation and its associated cytotoxic effects can be inhibited in the presence of the polyphenol (−)-epigallocatechin-3-gallate (EGCG). Potentially, amyloid formation plays a pivotal role in the AMP activity of uperin 3.5.

Results

Uperin 3.5 self assembly

The ability of several AMPs from Australian amphibians to form amyloid fibrils was assessed in vitro. From this initial screen, it was noticed that uperin 3.5 self assembles to form amyloid fibrils in buffered solutions at physiological pH. The fibril formation process was investigated by using several methods. Firstly, an in situ ThT fluorescence assay monitored the kinetics of fibril formation by uperin 3.5 (Figure 1 A). An increase in fluorescence was observed as a function of time; this is consistent with the formation of β-sheet-rich aggregates and a conversion from monomeric peptide to amyloid fibrils. Little to no lag phase was observed, and the elongation phase was complete within approximately 5 h. Furthermore, decreasing the concentration did not result in distinguishable differences in lag times, however, a reduction in fibril yield was observed (Figure S1 in the Supporting Information).

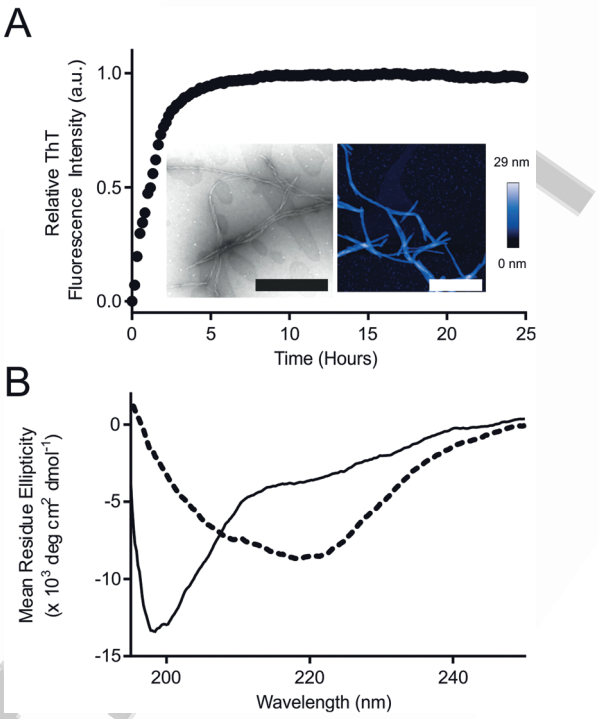

Figure 1. Amyloid fibril formation by uperin 3.5. A) In situ ThT fluorescence assay of fibril formation by uperin 3.5 at 37 °C in PBS. Representative data from three independent experiments performed in triplicate are shown. The insets show representative TEM and AFM images of the fibrillar species observed after 24 h (scale bars: 1 μm). B) Far-UV CD spectra of a freshly prepared 3 μM solution of uperin 3.5 (——) and a solution incubated at 37 °C for 5 h (-----).

The morphology of the resultant fibrils was analysed by TEM and AFM (Figure 1 A, inset). The fibrillar species produced are approximately 20 nm high and 400 nm in length, with characteristic coiled-coil ultrastructure. The secondary structure content of the resultant fibrils, when compared with the native peptide, was examined by using far-UV CD spectroscopy (Figure 1 B). During incubation of uperin 3.5, a transition occurred from a random-coil structure (with a CD spectrum displaying a characteristic ellipticity minimum at approximately 195 nm) to a structural ensemble comprising significant β-sheet conformation with a broad negative ellipticity maximum at approximately 218 nm, characteristic of amyloid fibrils. Some α-helical structure is also possibly present with broad minima at approximately 208 and 222 nm, indicative of the pathway to the final β-sheet-rich structure.

Modulation of uperin 3.5 secondary structure and self-assembly with 2,2,2-trifluoroethanol

TFE destabilises hydrophobic interactions within polypeptide chains and stabilises local hydrogen bonds between proximal residues in a polypeptide. Consequently, as a cosolvent it is capable of stabilising secondary structure where it has the propensity to form.[17] In buffered aqueous solution, uperin 3.5 exhibits a far-UV CD spectrum characteristic of a random-coil structure, however, addition of TFE (0–50 %, *v/v*) to native

uperin 3.5 showed that α-helical structure is induced in a concentration-dependent manner, as evidenced by the far-UV CD spectra, which show characteristic negative ellipticity maxima at approximately 210 and 220 nm (Figure 2A). Addition of TFE

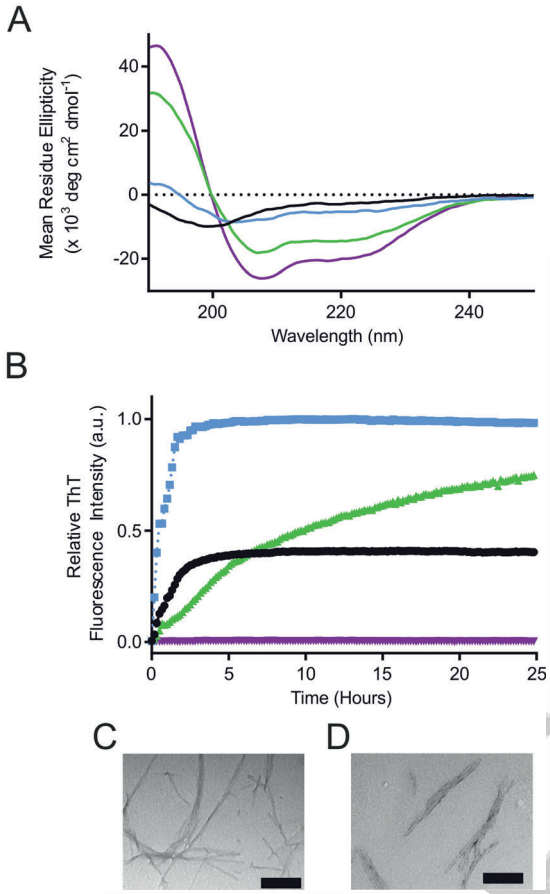

Figure 2. Effect of 2,2,2-trifluoroethanol on the conformation and aggregation of uperin 3.5. A) Far-UV CD spectrum of uperin 3.5 in PBS (——), and in the presence of 10 (——), 20 (——) and 50% (——) TFE. B) In situ ThT fluorescence assay showing the kinetics of fibril formation by uperin 3.5 (——), and in the presence of 10 (——), 20 (——) and 50% (——) TFE. Representative data from three independent experiments performed in triplicate are shown. TEM images of the fibrillar species produced by uperin 3.5 after incubation at 37 °C for 24 h in the presence of C) 10 and D) 20% TFE. Scale bars: 200 nm.

to the in-situ ThT fluorescence assay demonstrates that the presence of 10% (*v/v*) TFE enhances aggregation significantly, 20% (*v/v*) TFE only moderately enhances aggregation, and the addition of 50% (*v/v*) TFE ■■eliminates fibril formation (Figure 2B); this was confirmed by TEM imaging (data not shown) *OK?*■■. Fibril morphology is not affected significantly by the presence of TFE, as indicated by TEM imaging (Figure 2C and D).

Ion mobility–mass spectrometry analysis of prefilbrillar oligomers of uperin 3.5

Mass spectrometry is emerging as an important technique for studying early-stage peptide/protein oligomerisation, especially due to its unique ability to detect the lowly populated transient intermediate states occupied on the way to amyloid fibrils.[18] In order to study the self-assembly of uperin 3.5 by nanoelectrospray-ion mobility–MS (IM-MS), it was necessary to determine if the peptide was capable of forming amyloid fibrils in solutions of MS-compatible buffers. Thus, an in-situ ThT fluorescence assay was undertaken for a 100 μM solution of uperin 3.5 in 50 mM ammonium acetate (pH 6.9). The kinetics of fibril formation were not significantly different from those in phosphate buffer, and the morphology of the fibrils was also similar, as determined by TEM (data not shown).

The early-stage prefibrillar oligomeric states were studied by IM-MS by using freshly prepared peptide solutions, as the relative abundance of oligomeric species observed by IM-MS decreases as a function of aggregation time, most likely due to the higher-order oligomers being incorporated into fibrils.[19] Figure 3A shows the mass spectrum of uperin 3.5, with the oligomers (and their charge states) indicated. Oligomeric states up to a hexamer were observed in the IM-MS spectrum. The observed oligomers all adopted only one or two charge states

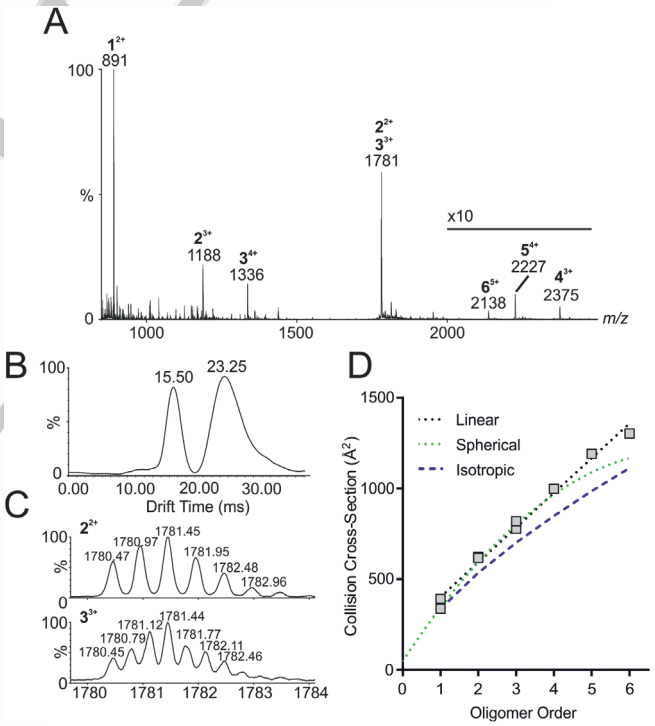

Figure 3. IM-MS analysis of uperin 3.5 oligomerisation. A) Mass spectrum of 100 μM uperin 3.5 in 50 mM NH_4OAc (pH 6.9). The peaks are labelled according to the number of peptides per oligomer, with their charge state indicated as a superscript. B) The arrival time distribution of isobaric ions with *m/z* 1781. The peaks show two oligomeric states that can be identified by their isotopic distributions. The 2^{2+} species has a longer drift time than the 3^{3+} species. C) The isotopic distributions for the 2^{2+} (top, arrival time of 23.25 ms) and 3^{3+} (bottom, arrival time of 15.50 ms) oligomers. D) Measured uperin 3.5 CCSs plotted as a function of the number of subunits in the oligomer. The blue dotted line displays estimated CCSs assuming an isotropic assembly process (here the CCS of the monomer is scaled by $n^{2/3}$, where n is the number of subunits in the oligomer),[20] and the green line corresponds to the expected CCSs for globular proteins, based on the average density of a protein (0.44 Da Å^{-13}).[21] The dotted line shows a linear regression analysis of the experimental data points, $r^2 = 0.99$.

upon ionisation; this indicates that they are of relatively compact, well-defined structures.

Importantly, IM-MS allows species of the same *m/z*, but different mass and charge to be separated; this is illustrated in Figure 3B, which shows the arrival time distribution (ATD) of ions with *m/z* 1781. Two different species are present, and separating them allows their respective isotopic distributions to be observed (Figure 3C). Generally, more highly charged oligomers have higher mobility, and therefore a shorter drift time. This is observed for uperin 3.5, with the trimer (+3 charge state) having a shorter drift time than the dimer (+2 charge state; Figure 3B, C).

IM-MS also permits the separation of ions with identical mass and *m/z*, but different conformations. Both doubly and triply charged monomer charge states were observed, with each charge state having both an expanded and compact conformation for the same mass species (Table S1). ATDs were extracted from the spectra for the oligomeric species observed. The drift times were converted to rotationally averaged collision cross-sections (CCS) by using a calibration protocol[22] and compared with those estimated for several theoretical models, such as those assuming an isotropic growth,[20] a model assuming a globular size (based on an average protein density of 0.44 Da Å^{-13}),[21] and an linear growth model[20] (Figure 3D and Table S1). As seen in Figure 3D, the CCS measurements indicate that oligomeric growth occurs in a directional fashion; this is consistent with a linear growth model.

Influence of uperin 3.5 on the viability of PC12 cells measured by MTT reduction

It is well known that the amyloidogenic forms of proteins display enhanced cytotoxicity relative to the unaggregated species.[10a–c] To assess this effect, the influence of native and fibrillar uperin 3.5 on the viability of cultured pheochromocytoma-12 (PC12) cells, a neuronal cell model,[23] was determined by using the methylthiazolyldiphenyl-tetrazolium bromide (MTT) assay.[23]

Treatment of cells with preincubated uperin 3.5, which had formed amyloid-like fibrils (as evidenced by ThT fluorescence and TEM imaging), caused a dose-dependent decrease in cell viability (Figure 4). In the main, this effect was not observed with native (un-incubated) peptide, as measured by the MTT assay. The native peptide forms caused a decrease in cell viability at high concentration (50 μM), most likely due to formation of aggregates in the culture medium.[23]

(−)-Epigallocatechin-3-gallate inhibits amyloid formation by uperin 3.5 and disassembles preformed fibrils

The polyphenol (−)-epigallocatechin-3-gallate (EGCG) and other related molecules have been the subject of much research due to their ability to inhibit amyloid formation by a variety of disease-related proteins.[24] The anti-aggregation efficacy of EGCG towards uperin 3.5 was monitored in an in situ ThT fluorescence assay. Uperin 3.5 (100 μM) was incubated at 37 °C in the presence of a fourfold molar excess of EGCG; this resulted in the complete mitigation of any time-dependent increase in ThT fluorescence (Figure 5A), thus implying that EGCG prevented fibril formation by uperin 3.5. Furthermore, addition of EGCG after the elongation phase resulted in a decrease in ThT fluorescence, indicative of fibril disassembly (Figure 5A). In addition, the change in aggregate morphology induced by EGCG was monitored by using TEM. The images show a redirection of fibril formation towards amorphous aggregation (Figure 5B–D).

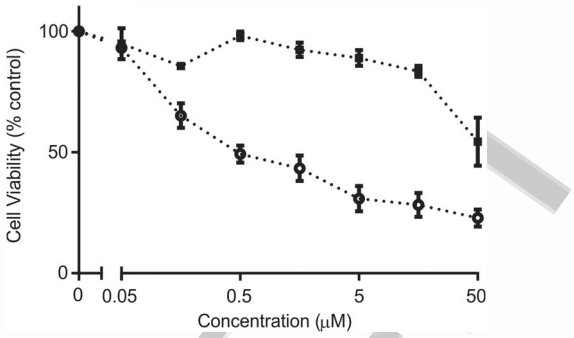

Figure 4. Concentration-dependent influence on cell viability of native and fibrillar uperin 3.5 as measured by MTT reduction. Uperin 3.5 was dissolved in PBS, then either frozen in its native form or incubated for 24 h at 37 °C to induce fibril formation. Native (■) and fibrillar (○) forms of uperin 3.5 were then added to the cell culture medium (RPMI 1640) of the PC12 cells, and they were incubated for 48 h. Cell viability was assessed by using the MTT assay. Values are presented as percentage of cell survival compared with a control ± SEM of three independent experiments, each with six replicates.

EGCG also prevented the formation of the higher-order oligomers observed by IM-MS (Figure 3), whereby multiple copies of EGCG were observed to be bound to monomeric uperin 3.5 (Figure S3). This is typical of the inhibition of fibril formation attributed to nonspecific binding to the monomeric peptide, rather than EGCG binding at a specific site.

Finally, to assess the cytoprotective activity of EGCG, PC12 cells were treated with uperin 3.5 preincubated at 37 °C for 24 h with and without EGCG. Following incubation of the treated cells for 48 h, cell viability was assessed by MTT reduction. Treatment with EGCG alone did not result in a change in cell viability. Significant protection from the amyloid-associated decrease in cell viability, as measured by the MTT reduction, was observed when uperin 3.5 was coincubated with EGCG (Figure 5E).

Discussion

Amyloid fibril formation by uperin 3.5

In this work we have comprehensively investigated the amyloidogenicity of the amphibian AMP uperin 3.5, which forms amyloid fibrils rapidly under physiological conditions (Figure 1), a process that might be involved in its biological function.

Solution conditions are well known to affect ■■the fibril-formation kinetics of *OK?*■■ peptides and proteins. For example, the presence of co-solvents, high temperatures and extreme pH, alter the kinetics and extent of aggregation.[25] Tri-

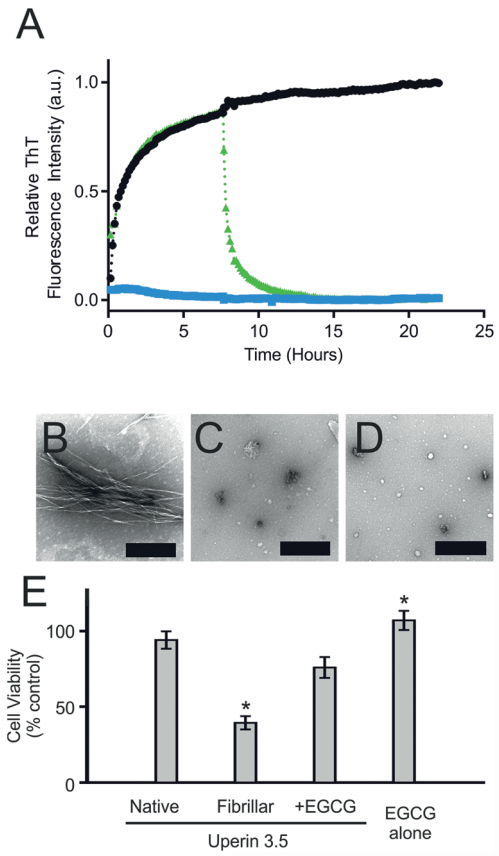

Figure 5. EGCG inhibits amyloid-like fibril formation by uperin 3.5. A) In situ ThT fluorescence assay of fibril formation by uperin 3.5 (●) and in the presence of EGCG (■). Addition of EGCG after the elongation phase (▲) results in a decrease in ThT fluorescence. Representative data are shown from three independent experiments performed in triplicate. TEM images of the species produced when uperin 3.5 was B) incubated for 24 h at 37 °C in PBS, C) incubated in the presence of EGCG and D) incubated, followed by the addition of EGCG after the elongation phase. Scale bars: 500 nm. E) MTT cytotoxicity assay of PC12 cells treated with 1 μM uperin 3.5 preincubated at 37 °C for 24 h in RPMI 1640 medium in the presence and absence of EGCG. Treatment with EGCG alone did not affect cytotoxicity. Values are presented as percentage of cell survival compared with a control ± SEM of three independent experiments, each with six replicates (* indicates $P < 0.05$).

fluoroethanol is a well-known organic cosolvent that has the ability to induce secondary structure, in particular helical conformation, where it has the propensity to form.[17b] Additionally, TFE mimics a membrane environment.[26] A variety of proteins and peptides form fibrils in the presence of TFE.[25b, 27]

It is apparent that adding TFE to uperin 3.5-containing solutions triggers the conversion from a random-coil conformation to an α-helical structure, as evidenced by the far-UV CD spectra in Figure 2A, which show overall enhanced helicity in uperin 3.5 when increasing amounts of TFE are added. Importantly, the far-UV CD spectra demonstrate that in 10 and 20% (*v*/*v*) TFE, a small degree of α-helical secondary structure is induced; this increases upon addition of 50% (*v*/*v*) TFE. Despite this, amyloid fibrils are still formed in both 10 and 20% aqueous TFE solutions, but this process is inhibited in 50% aqueous TFE (Figure 2B–D). Consistent with this, the NMR-derived structure of the closely related peptide uperin 3.6 is helical in 50% aqueous TFE.[28] However, uperin 3.6 has no propensity to form fibrils in aqueous solution or at any concentration of TFE (unpublished observations). From these data, it can be concluded that the degree of α-helical structure present in the uperin 3.5 peptide precursor, which depends on the concentration of TFE, plays a role in the peptide's fibril formation. Low concentrations of TFE, which introduce limited, dynamic helical structure, result in enhanced fibril kinetics and yield, whereas at higher concentrations of TFE, at which the peptide is trapped in a helical state, fibril formation does not proceed. Similar effects of low amounts of TFE on fibril formation have been observed for many other peptides and proteins. For example, we observed such behaviour for eye-lens crystallin proteins in 10% TFE at pH 2.0.[29] Given that uperin 3.5 adopts a predominantly α-helical structure in the presence of the membrane mimetic TFE, it is likely that the membrane environment plays a role in the aggregation of uperin 3.5.

Recently, IM-MS was used to investigate the self-assembly processes of numerous amyloidogenic proteins and peptides. The technique is ideally suited to this endeavour as it possible to characterise heterogeneous populations with relative ease, unlike many other commonly used biophysical methods.[18–19, 30] The mass spectrum shown in Figure 3A indicates that oligomeric species of uperin 3.5 from monomer to hexamer can be observed under the conditions used.

Calibrated CCS values were plotted as a function of oligomer number to give insight into the self-assembly process of the oligomers (Figure 3D). From these data, it is possible to determine whether the self-assembly proceeds by a highly directional fibrillar process whereby the relationship between CCS and oligomer number exhibits a linear correlation,[20] in contrast to the CCSs that would be expected for a spatially isotropic self-assembly or a globular structure with a typical density. It is apparent for the small number of oligomers observed that a linear regression line can be fitted to the CCS data (Figure 3D), that is, these data do not agree with the expected CCS values for isotropic and spherical assemblies. It is concluded that a highly directional, fibrillar type self-assembly process predominates for uperin 3.5 in the early stages of its aggregation. Similarly, elongated, rather than globular, oligomers were also observed by IM-MS for the type II diabetes-associated peptide amylin[19a] and for β2-microglobulin, the protein associated with dialysis-related amyloidosis.[31] Conversely, a study of amyloid-β(1–42) oligomerisation by IM-MS led to a self-assembly model with more complex architectures, notably ring-like hexamers and a higher-order assembly comprising two stacked hexameric units.[32]

For disease-related fibril-forming peptides and proteins, there is a correlation between the induction of cytotoxicity and the formation of the fibrillar state that is proposed to be due to the presence of prefibrillar aggregates,[5a, 8a, c, e–g, 33] or, in some instances, the fibrils themselves.[10a, 13a, 21, 24c] Conversely, the non-aggregated forms of the protein have limited cytotoxicity. Here, both the native and fibrillar species of uperin 3.5 caused a concentration-dependent decrease in PC12 cell viability (measured by MTT reduction; Figure 4); however, the effect of fibrillar uperin 3.5 was significantly enhanced at lower con-

centrations compared with that of the native peptide. For example, at 0.5 μM, fibrillar uperin 3.5 reduced cell viability to 43 ± 5%, compared with 92 ± 3% for the native peptide. It has been previously demonstrated that the integral nature of fibrillar species is maintained in cell culture media, and that fibril formation still proceeds, albeit at a reduced rate.[10a] The effect on cell viability of native uperin 3.5 at high concentrations most probably arises from the formation of fibrillar species in the culture medium, due to the high aggregation propensity of uperin 3.5, which lacks a lag phase.[10a]

Flavonoids, such as EGCG from green tea, inhibit fibrillogenesis by amyloid-forming proteins both in vitro and in vivo. In particular, EGCG inhibits fibril formation by numerous disease- and non-disease-related amyloid-fibril-forming proteins such as amyloid-β, α-synuclein and huntingtin, amongst others.[10c, d, 19a, 24c, 34] The mechanisms by which EGCG and other flavonoids achieve this are not well understood, and it is proposed that many different types of intermolecular contacts might mediate this inhibition.[35]

It is evident from the results presented herein that EGCG has a similar effect in preventing aggregation by uperin 3.5. When uperin 3.5 was incubated in the presence of four molar equivalents of EGCG, there was a significant reduction in the maximum ThT fluorescence observed (Figure 5). These results were confirmed by TEM analysis to determine the effects on morphology. It is evident that co-incubation with EGCG results in the formation of compact spherical oligomers, as opposed to the fibrillar species observed in the absence of EGCG (Figure 5 B–D).

In addition, EGCG has the ability to disaggregate and remodel the amyloid fibrils formed by a number of disease-related proteins.[36] The data obtained here show that EGCG remodels uperin 3.5, that the structures produced are not amyloid fibrils, and that they closely represent the structures produced when EGCG is added at the start of the aggregation process (Figure 5 A).

Finally, it was demonstrated that coincubation of uperin 3.5 with EGCG prevents the decrease in cell viability in PC12 cells that is associated with the amyloidogenic uperin 3.5 species (Figure 5 E). It should be noted that EGCG and other polyphenols have properties that might also contribute to the prevention of uperin 3.5 toxicity. These include their ability to scavenge radicals, reduce reactive oxidative species and to chelate metal ions.[35a, 37] However, many other fibril-forming proteins that give rise to similar morphologies upon EGCG treatment have been studied, and in all instances, the soluble spherical aggregates that are formed have been described as non-cytotoxic.[10c, d, 19a, 24c, 34]

Relevance of amyloid fibril formation to the AMP activity of uperin 3.5

Much work in the area of AMPs is focussed on determining their structures and modes of action as a means of implementing and improving peptide antibiotics as therapeutics. It has been proposed that the amyloidogenic nature of some AMPs, namely the temporins B and L, means that soluble peptide oligomers might be responsible for their antimicrobial activity, and that the membrane might mediate amyloid formation. In other words, there is an association between the toxic function of the AMP and its ability to aggregate.[6] Consequently, there could be a common mechanism of action of AMPs that have the propensity to form amyloid fibrils.

Interestingly, it has been proposed that the oligomers formed by amyloidogenic AMPs in a membrane might have a mechanism of membrane permeabilisation different from both the canonical barrel-stave and toroidal pore mechanisms. This mechanism is termed the "leaky slit" model, and is based on the formation of toxic oligomers in the bilayer.[13a, 15a, 38] This results in the formation of transmembrane linear, amphipathic arrays of peptides that arrange with the hydrophobic faces interacting with the bilayer. Consequently, the hydrophilic face forces the lipids on this side to adopt a curved structure that joins the inner and outer leaflets of the membrane, resulting in membrane disruption.

Torrent et al.[6b] have observed that the amino acid sequences of aggregation-prone peptides and AMPs are closely correlated at the amino acid level in their individual aggregation propensity and antimicrobial index. Furthermore, the conversion from aggregation-prone peptides to AMPs can be accomplished by the strategic insertion of positively charged lysine or arginine amino acids into the peptide sequence to facilitate binding to the negatively charged phospholipids of the bacterial cell membrane. Intriguingly, of all the groups of organisms studied, frog-skin AMPs have the greatest aggregation tendency. ■■Torrent's group's *OK?*■■ data imply that AMPs evolved from aggregation-prone peptides through the selective incorporation of positively charged amino acids.

The apparent functional and evolutionary link between the fibril formation of AMPs, such as uperin 3.5, and their mechanism of antimicrobial action requires further research. It is conceivable that research of this nature will provide significant insights into the mechanism of disease-related amyloid cytotoxicity.[15]

Conclusion

Many AMPs have the inherent ability to form amyloid structures. In this work, the amyloidogenicity of uperin 3.5 was investigated, and its ability to form amyloid fibrils was compared with that of other disease-related proteins and peptides. It is apparent that uperin 3.5 formed amyloid fibrils with rapid kinetics, as the process lacks a lag phase. The resultant fibrils were of a typical coiled-coil ultrastructure, which is rich in β-sheet content. Addition of the secondary-structure-inducing cosolvent TFE enhanced fibril formation kinetics when small quantities were present, but inhibited them at higher concentrations. The flexible α-helical structure induced at low TFE concentrations can readily convert to β-sheet-rich amyloid. However, at higher concentrations, the more rigid, well-defined α-helical secondary structure is unable to convert. Fibrillar species of uperin 3.5 were cytotoxic to cultured neuronal cells, in a similar fashion to other disease-related amyloid species. This supports the notion that the generic amyloid structure is toxic,

and that the effect is sequence independent. Furthermore, EGCG, a flavonoid from green tea, inhibited uperin 3.5 fibril formation, remodelled the mature fibrils and prevented the cytotoxicity associated with uperin 3.5 fibril formation.

These data provide significant evidence for the structural similarities between amyloid fibrils formed by uperin 3.5 and those of disease-related proteins. Additionally, they provide further support for the notion that fibrils formed by AMPs possess properties similar to those of disease-related amyloidogenic proteins. Our work adds to the growing body of literature that suggests that mechanistic investigations of AMPs that form amyloid structures can provide significant insight into the means by which disease-related amyloid species elicit their sometimes devastating effects.

Experimental Section

Materials: Unless otherwise stated, reagents were purchased from Sigma–Aldrich. Peptides were synthesized by GenScript Corp. (Piscataway, NJ, USA) or GenicBio (Shanghia, China) from L-amino acids by using solid-phase methods and were greater than 80% pure, respectively, as determined by HPLC and ESI-MS (Supporting Information).

In-situ thioflavin T fluorescence assays: Samples for the in-situ ThT assay were prepared by diluting concentrated peptide stock solutions (typically 1 mM in H_2O for uperin 3.5) into phosphate-buffered saline (PBS, pH 7.4) solution at the appropriate concentrations (100 μM uperin 3.5). The final concentration of ThT in the samples was 10 μM. Samples were incubated at 37 °C in black μClear 96-microwell plates (Greiner Bio-One, Stonehouse, UK) that were sealed with clear film (Sigma–Aldrich) to prevent evaporation. The ThT fluorescence intensities of the samples were recorded on a Fluostar Optima plate reader (BMG Labtech, Offenburg, Germany) fitted with 440/490 nm excitation/emission filters. Data were normalized by plotting the relative change in ThT fluorescence [arbitrary units] between the initial and final fluorescence readings.

Transmission electron microscopy: Aliquots (5 μL) were taken from samples after the ThT fluorescence assay and applied to the surface of carbon-coated 400-mesh nickel TEM grids (ProSciTech, Townsville, Australia). The grids were washed with milliQ H_2O (3× 10 μL) and negatively stained with uranyl acetate solution (2% *w/v*, 10 μL). Samples were viewed by using a Philips CM100 transmission electron microscope (Philips) or a Tecnai G2 Spirit transmission electron microscope (FEI Company, Hillsboro, OR, USA).

Atomic force microscopy: AC-mode AFM images were obtained by using a Nanowizard III AFM (JPK Instruments AG, Berlin, Germany) installed on a Nikon TE-2000 inverted epifluorescence microscope. Cantilevers used were Bruker NCHV model, with a nominal resonant frequency and spring constant of 320 kHz and 42 N m^{-1}, respectively. Line rates of 1–3 Hz were used, and images were processed by using the JPK instrumental software. Samples for AFM were placed as solution onto freshly-cleaved mica discs and dried; imaging was performed in air.

Circular dichroism spectroscopy: Far-UV CD spectra were recorded on a J-815 CD spectropolarimeter (Jasco, MD, USA) by using a 0.1 cm path-length cuvette and averaging of five scans. The buffer contribution was subtracted for each experiment. Spectra were recorded at 25 °C.

Ion mobility-mass spectrometry: Uperin 3.5 (100 μM) was dissolved in NH_4OAc (20 mM). IM-MS spectra were acquired on a Synapt HDMS system (Waters)[39] by using nanoelectrospray ionisation (nanoESI) in positive-ion mode. The sample was introduced by using platinum-coated borosilicate capillary needles that were prepared in-house. Instrument parameters were optimised to remove adducts whilst preserving noncovalent interactions, and were typically as follows: capillary voltage: 1.7 kV, cone voltage: 100 V, trap collision energy: 10 V, source temperature: 50 °C, backing pressure: 3.5 mbar, IMS cell pressure (N_2): 0.5 mbar, travelling wave velocity: ■■300 m s^{-1} OK?■■, travelling wave height: 8–10 V. Drift-time measurements obtained from the Synapt HDMS were normalised for charge state and calibrated to give a rotationally averaged collision cross-section (CCS) according to a described procedure.[22]

Cell culture: PC12 cells were cultured in RPMI 1640 medium (Invitrogen) supplemented with 5% (*v/v*) foetal bovine serum, L-glutamine (2 mM), antibiotic/antimicotic mixture (100 mg mL^{-1} penicillin and 100 units mL^{-1} streptomycin) and nonessential amino acids (100 units mL^{-1}). Cells were grown in uncoated ■■75 cm^2 *"cm³"?* ■■ plastic flasks at 37 °C in a 5% CO_2-humidified incubator, and subcultured every 3–7 days.

MTT assay: Cells were seeded the day prior to treatment at a density of 2×10^4 cells per well in a 96-well plate. Peptides (500 μM) were dissolved in PBS and either snap-frozen on dry ice and stored at −80 °C (nonfibrillar) or incubated at 37 °C for 24 h. The samples were diluted in PBS to the required concentrations (10 μL) and added to full-serum RPMI 1640 (100 μL). After a treatment time of 72 h, the culture medium was removed, and the cells were incubated with serum-free medium containing methylthiazolyldiphenyl-tetrazolium bromide (0.25 mg mL^{-1}) for 3 h. The medium was removed and replaced with dimethyl sulfoxide (100 μL), and the absorbance of the resultant formazan solution was measured at 560 nm by using a BMG Polarstar microplate reader (BMG Labtech). Cell viability was assessed as percentage absorbance relative to the vehicle control (PBS only) as the mean of three independent experiments (six replicates per experiment). Where appropriate, differences between data sets were evaluated by performing analysis of variance (ANOVA) followed by Dunnett's test. A level of $p<0.05$ was considered to be significant.

Acknowledgements

The authors would like to acknowledge financial support from the Australian Research Council and the National Health and Medical Research Council of Australia.

Keywords: aggregation · amyloid · antimicrobial peptides · mass spectrometry · uperin

[1] a) M. Zasloff, *Nature* **2002**, *415*, 389–395; b) A. Cederlund, G. H. Gudmundsson, B. Agerberth, *FEBS J.* **2011**, *278*, 3942–3951.
[2] K. A. Brogden, *Nat. Rev. Microbiol.* **2005**, *3*, 238–250.
[3] a) M. A. Apponyi, T. L. Pukala, C. S. Brinkworth, V. M. Maselli, J. H. Bowie, M. J. Tyler, G. W. Booker, J. C. Wallace, J. A. Carver, F. Separovic, J. Doyle, L. E. Llewellyn, *Peptides* **2004**, *25*, 1035–1054; b) T. L. Pukala, J. H. Bowie, V. M. Maselli, I. F. Musgrave, M. J. Tyler, *Nat. Prod. Rep.* **2006**, *23*, 368–393; c) J. H. Bowie, F. Separovic, M. J. Tyler, *Peptides* **2012**, *37*, 174–188.
[4] a) P. Vlieghe, V. Lisowski, J. Martinez, M. Khrestchatisky, *Drug Discovery Today* **2010**, *15*, 40–56; b) C. D. Fjell, J. A. Hiss, R. E. W. Hancock, G. Schneider, *Nat. Rev. Drug Discovery* **2012**, *11*, 37–51; c) N. Y. Yount, M. R.

Yeaman, *Annu. Rev. Pharmacol. Toxicol.* **2012**, *52*, 337 – 360; d) B. M. Peters, M. E. Shirtliff, M. A. Jabra-Rizk, *PLoS Pathog.* **2010**, *6*, e1001067.

[5] a) G. Diamond, N. Beckloff, A. Weinberg, K. O. Kisich, *Curr. Pharm. Des.* **2009**, *15*, 2377 – 2392; b) L. T. Nguyen, E. F. Haney, H. J. Vogel, *Trends Biotechnol.* **2011**, *29*, 464 – 472.

[6] a) A. K. Mahalka, P. K. Kinnunen, *Biochim. Biophys. Acta. Biomembr.* **2009**, *1788*, 1600 – 1609; b) M. Torrent, J. Valle, M. V. Nogues, E. Boix, D. Andreu, *Angew. Chem. Int. Ed.* **2011**, *50*, 10686 – 10689; *Angew. Chem.* **2011**, *123*, 10874 – 10877; c) M. Torrent, D. Andreu, M. V. Nogues, E. Boix, *PLoS ONE* **2011**, *6*, e16968.

[7] T. X. Hoang, L. Marsella, A. Trovato, F. Seno, J. R. Banavar, A. Maritan, *Proc. Natl. Acad. Sci. USA* **2006**, *103*, 6883 – 6888.

[8] a) M. Stefani, *Prog. Neurobiol.* **2012**, *99*, 226 – 245; b) R. Kayed, C. Lasagna-Reeves, *J. Alzheimer's Dis.* **2012**, *33*, S67 – S78; c) S. M. Butterfield, H. A. Lashuel, *Angew. Chem. Int. Ed.* **2010**, *49*, 5628 – 5654; *Angew. Chem.* **2010**, *122*, 5760 – 5788; d) M. Bucciantini, E. Giannoni, F. Chiti, F. Baroni, L. Formigli, J. Zurdo, N. Taddei, G. Ramponi, C. M. Dobson, M. Stefani, *Nature* **2002**, *416*, 507 – 511; e) M. Sakono, T. Zako, *FEBS J.* **2010**, *277*, 1348 – 1358; f) K. Berthelot, C. Cullin, S. Lecomte, *Biochimie* **2013**, *95*, 12 – 19; g) F. Chiti, C. M. Dobson, *Annu. Rev. Biochem.* **2006**, *75*, 333 – 366.

[9] S. Campioni, B. Mannini, M. Zampagni, A. Pensalfini, C. Parrini, E. Evangelisti, A. Relini, M. Stefani, C. M. Dobson, C. Cecchi, F. Chiti, *Nat. Chem. Biol.* **2010**, *6*, 140 – 147.

[10] a) M. Bucciantini, D. Nosi, M. Forzan, E. Russo, M. Calamai, L. Pieri, L. Formigli, F. Quercioli, S. Soria, F. Pavone, *FASEB J.* **2012**, *26*, 818 – 831; b) A. L. Gharibyan, V. Zamotin, K. Yanamandra, O. S. Moskaleva, B. A. Margulis, I. A. Kostanyan, L. A. Morozova-Roche, *J. Mol. Biol.* **2007**, *365*, 1337 – 1349; c) V. Novitskaya, O. V. Bocharova, I. Bronstein, I. V. Baskakov, *J. Biol. Chem.* **2006**, *281*, 13828 – 13836; d) L. Milanesi, T. Sheynis, W. F. Xue, E. V. Orlova, A. L. Hellewell, R. Jelinek, E. W. Hewitt, S. E. Radford, H. R. Saibil, *Proc. Natl. Acad. Sci. USA* **2012**, *109*, 20455 – 20460.

[11] M. F. Engel, L. Khemtémourian, C. C. Kleijer, H. J. Meeldijk, J. Jacobs, A. J. Verkleij, B. De Kruijff, J. A. Killian, J. W. Höppener, *Proc. Natl. Acad. Sci. USA* **2008**, *105*, 6033 – 6038.

[12] a) T. Härd, C. Lendel, *J. Mol. Biol.* **2012**, *424*, 441 – 465; b) K. A. DaSilva, J. E. Shaw, J. McLaurin, *Exp. Neurol.* **2010**, *223*, 311 – 321; c) K. L. Sciarretta, D. J. Gordon, S. C. Meredith, *Methods Enzymol.* **2006**, *413*, 273 – 312.

[13] a) Y. Shai, *Biopolymers* **2002**, *66*, 236 – 248; b) K. Matsuzaki, *Biochim. Biophys. Acta Biomembr.* **2007**, *1768*, 1935 – 1942.

[14] R. Gössler-Schöfberger, G. Hesser, M. Muik, C. Wechselberger, A. Jilek, *FEBS J.* **2009**, *276*, 5849 – 5859.

[15] a) F. Harris, S. R. Dennison, D. A. Phoenix, *FASEB J.* **2012**, *26*, 1776 – 1781; b) M. Zhang, J. Zhao, J. Zheng, *Soft Matter* **2014**, *10*, 7425 – 7451.

[16] A. M. Bradford, J. H. Bowie, M. J. Tyler, J. C. Wallace, *Aust. J. Chem.* **1996**, *49*, 1325 – 1331.

[17] a) D. P. Hong, M. Hoshino, R. Kuboi, Y. Goto, *J. Am. Chem. Soc.* **1999**, *121*, 8427 – 8433; b) M. Buck, *Q. Rev. Biophys.* **1998**, *31*, 297 – 355.

[18] a) D. M. Williams, T. L. Pukala, *Mass Spectrom. Rev.* **2013**, *32*, 169 – 187; b) L. A. Woods, S. E. Radford, A. E. Ashcroft, *Biochim. Biophys. Acta Proteins Proteomics* **2013**, *1834*, 1257 – 1268.

[19] a) L. M. Young, P. Cao, D. P. Raleigh, A. E. Ashcroft, S. E. Radford, *J. Am. Chem. Soc.* **2014**, *136*, 660 – 670; b) C. A. Scarff, B. Almeida, J. Fraga, S. Macedo-Ribeiro, S. E. Radford, A. E. Ashcroft, *Mol. Cell. Proteomics* **2015**, *14*, 1241 – 1253.

[20] C. Bleiholder, N. F. Dupuis, T. Wyttenbach, M. T. Bowers, *Nat. Chem.* **2011**, *3*, 172 – 177.

[21] K. Lorenzen, A. S. Olia, C. Uetrecht, G. Cingolani, A. J. Heck, *J. Mol. Biol.* **2008**, *379*, 385 – 396.

[22] a) B. T. Ruotolo, J. L. P. Benesch, A. M. Sandercock, S.-J. Hyung, C. V. Robinson, *Nat. Protoc.* **2008**, *3*, 1139 – 1151; b) M. F. Bush, Z. Hall, K. Giles, J. Hoyes, C. V. Robinson, B. T. Ruotolo, *Anal. Chem.* **2010**, *82*, 9557 – 9565.

[23] F. C. Dehle, H. Ecroyd, I. F. Musgrave, J. A. Carver, *Cell Stress Chaperones* **2010**, *15*, 1013 – 1026.

[24] a) D. E. Ehrnhoefer, J. Bieschke, A. Boeddrich, M. Herbst, L. Masino, R. Lurz, S. Engemann, A. Pastore, E. E. Wanker, *Nat. Struct. Mol. Biol.* **2008**, *15*, 558 – 566; b) D. E. Ehrnhoefer, M. Duennwald, P. Markovic, J. L. Wacker, S. Engemann, M. Roark, J. Legleiter, J. L. Marsh, L. M. Thompson, S. Lindquist, P. J. Muchowski, E. E. Wanker, *Hum. Mol. Genet.* **2006**, *15*, 2743 – 2751; c) S. A. Hudson, H. Ecroyd, F. C. Dehle, I. F. Musgrave, J. A. Carver, *J. Mol. Biol.* **2009**, *392*, 689 – 700.

[25] a) S. Goda, K. Takano, K. Yutani, Y. Yamagata, R. Nagata, H. Akutsu, S. Maki, K. Namba, *Protein Sci.* **2000**, *9*, 369 – 375; b) M. R. Krebs, D. K. Wilkins, E. W. Chung, M. C. Pitkeathly, A. K. Chamberlain, J. Zurdo, C. V. Robinson, C. M. Dobson, *J. Mol. Biol.* **2000**, *300*, 541 – 549; c) L. Nielsen, R. Khurana, A. Coats, S. Frokjaer, J. Brange, S. Vyas, V. N. Uversky, A. L. Fink, *Biochemistry* **2001**, *40*, 6036 – 6046; d) D. E. Otzen, *Curr. Protein Pept. Sci.* **2010**, *11*, 355 – 371.

[26] L. Chaloin, P. Vidal, A. Heitz, N. Vanmau, J. Mery, G. Divita, F. Heitz, *Biochemistry* **1997**, *36*, 11179 – 11187.

[27] a) W. Liu, J. M. Prausnitz, H. W. Blanch, *Biomacromolecules* **2004**, *5*, 1818 – 1823; b) F. Chiti, P. Webster, N. Taddei, A. Clark, M. Stefani, G. Ramponi, C. M. Dobson, *Proc. Natl. Acad. Sci. USA* **1999**, *96*, 3590 – 3594; c) V. L. Anderson, T. F. Ramlall, C. C. Rospigliosi, W. W. Webb, D. Eliezer, *Proc. Natl. Acad. Sci. USA* **2010**, *107*, 18850 – 18855; d) Y. Fezoui, D. B. Teplow, *J. Biol. Chem.* **2002**, *277*, 36948 – 36954.

[28] B. C. S. Chia, J. A. Carver, T. D. Mulhern, J. H. Bowie, *J. Pept. Res.* **1999**, *54*, 137 – 145.

[29] S. Meehan, Y. Berry, B. Luisi, C. M. Dobson, J. A. Carver, C. E. MacPhee, *J. Biol. Chem.* **2004**, *279*, 3413 – 3419.

[30] a) A. E. Ashcroft, *J. Am. Soc. Mass Spectrom.* **2010**, *21*, 1087 – 1096; b) L. M. Young, J. C. Saunders, R. A. Mahood, C. H. Revill, R. J. Foster, L. H. Tu, D. P. Raleigh, S. E. Radford, A. E. Ashcroft, *Nat. Chem.* **2015**, *7*, 73 – 81.

[31] D. P. Smith, S. E. Radford, A. E. Ashcroft, *Proc. Natl. Acad. Sci. USA* **2010**, *107*, 6794 – 6798.

[32] S. L. Bernstein, N. F. Dupuis, N. D. Lazo, T. Wyttenbach, M. M. Condron, G. Bitan, D. B. Teplow, J. E. Shea, B. T. Ruotolo, C. V. Robinson, M. T. Bowers, *Nat. Chem.* **2009**, *1*, 326 – 331.

[33] a) S. T. Steinborner, G. J. Currie, J. H. Bowie, J. C. Wallace, M. J. Tyler, *J. Pept. Res.* **1998**, *51*, 121 – 126; b) M. Fändrich, *J. Mol. Biol.* **2012**, *421*, 427 – 440.

[34] S. A. Mandel, T. Amit, O. Weinreb, L. Reznichenko, M. B. Youdim, *CNS Neurosci. Ther.* **2008**, *14*, 352 – 365.

[35] a) Y. Porat, A. Abramowitz, E. Gazit, *Chem. Biol. Drug Des.* **2006**, *67*, 27 – 37; b) Y. Porat, Y. Mazor, S. Efrat, E. Gazit, *Biochemistry* **2004**, *43*, 14454 – 14462; c) D. Cao, Y. Zhang, H. Zhang, L. Zhong, X. Qian, *Rapid Commun. Mass Spectrom.* **2009**, *23*, 1147 – 1157.

[36] a) J. Bieschke, J. Russ, R. P. Friedrich, D. E. Ehrnhoefer, H. Wobst, K. Neugebauer, E. E. Wanker, *Proc. Natl. Acad. Sci. USA* **2010**, *107*, 7710 – 7715; b) F. Meng, A. Abedini, A. Plesner, C. B. Verchere, D. P. Raleigh, *Biochemistry* **2010**, *49*, 8127 – 8133; c) I. R. Chandrashekaran, C. G. Adda, C. A. MacRaild, R. F. Anders, R. S. Norton, *Arch. Biochem. Biophys.* **2011**, *513*, 153 – 157; d) P. Cao, D. P. Raleigh, *Biochemistry* **2012**, *51*, 2670 – 2683.

[37] a) D. Chen, V. Milacic, M. S. Chen, S. B. Wan, W. H. Lam, C. Huo, K. R. Landis-Piwowar, Q. C. Cui, A. Wali, T. H. Chan, Q. P. Dou, *Histol. Histopathol.* **2008**, *23*, 487 – 496; b) H. Shoval, D. Lichtenberg, E. Gazit, *Amyloid* **2007**, *14*, 73 – 87.

[38] a) H. Zhao, R. Sood, A. Jutila, S. Bose, G. Fimland, J. Nissen-Meyer, P. K. Kinnunen, *Biochim. Biophys. Acta Biomembr.* **2006**, *1758*, 1461 – 1474; b) P. K. J. Kinnunen, *Open Biol. J.* **2009**, *2*, 163 – 175.

[39] S. D. Pringle, K. Giles, J. L. Wildgoose, J. P. Williams, S. E. Slade, K. Thalassinos, R. H. Bateman, M. T. Bowers, J. H. Scrivens, *Int. J. Mass Spectrom.* **2007**, *261*, 1 – 12.

Manuscript received: October 7, 2015

Final article published: ■■ ■■, 0000

Frog-spawned fibrils: In solution, the AMP uperin 3.5 rapidly forms amyloid fibrils that are toxic to model neuronal cells. Mechanistically, the fibrils proceed via an α-helical intermediate and can be inhibited by the polyphenol EGCG. Several oligomeric states have been identified by ion-mobility MS in solution. A link between amyloid formation and AMP activity is mooted.

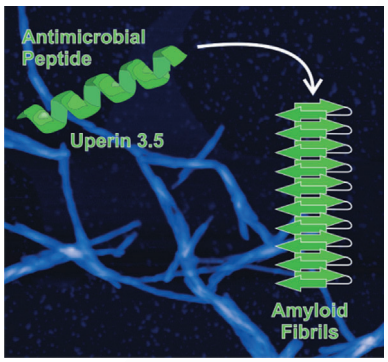

A. N. Calabrese, Y. Liu, T. Wang, I. F. Musgrave, T. L. Pukala, R. F. Tabor, L. L. Martin, J. A. Carver,* J. H. Bowie*

■■ – ■■

The Amyloid-Fibril-Forming Properties of the Amphibian Antimicrobial Peptide Uperin 3.5

Please check that the ORCID identifiers listed below are correct. We encourage all authors to provide an ORCID identifier for each coauthor. ORCID is a registry that provides researchers with a unique digital identifier. Some funding agencies recommend or even require the inclusion of ORCID IDs in all published articles, and authors should consult their funding agency guidelines for details. Registration is easy and free; for further information, see http://orcid.org/.

Antonio N. Calabrese
Yanqin Liu
Tianfang Wang
Ian F. Musgrave
Tara L. Pukala
Rico F. Tabor
Lisandra L. Martin
John A. Carver
John H. Bowie